# Low-Z perturbative impurity transport and microstability analysis on MAST

S. S. Henderson[1], L. Garzotti[2], F. J. Casson[3], D. Dickinson[2], M. O'Mullane[1], A. Patel[2], C. M. Roach[2], H. P. Summers[1], M. Valovič[2] and the MAST team

[1] *University of Strathclyde, Department of Physics, Glasgow, UK*

[2] *EURATOM/CCFE Fusion Association, Culham Science Centre, Abingdon, UK*

[3] *Max-Planck-Institut für Plasmaphysik, IPP-EURATOM Association, Garching, Germany*

## Introduction

Experiments have been carried out on MAST in an attempt to characterise the particle transport of low-Z impurities during typical plasma scenarios. It is important to understand the neoclassical and turbulent diffusivity ($D_Z$) and convective velocity ($V_Z$) to avoid fuel dilution and enhanced energy loss due to enhanced bremsstrahlung and line emission on next generation spherical tokamaks such as MAST-U. In this paper, we present the first experimental transport coefficient measurements for carbon and helium on MAST using visible charge exchange recombination (CXR) spectroscopy. Comparing these results to the neoclassical code, NCLASS [1], gives insight into the radial regions that must be dominated by turbulence. Linear gyrokinetic simulations using codes GS2 [2] and GKW [3] are used to understand microstability in those regions. Lastly, the dimensionless impurity density profile peaking factor is estimated from quasi-linear theory and compared to the experimental values.

## Experimental Setup

Carbon and helium are both intrinsic to MAST with typical unperturbed densities in the region $6n_c/n_e < 0.02$ and $2n_{he}/n_e < 0.2$. The 50 ms impurity puffs, characterised by $[1.7 - 2.7]$ $x10^{19}$ of $CD_4$ and He gas respectively, are injected into the plasma via the inboard fuelling valve on MAST. To obtain the perturbed the impurity density evolution, discharges with and without impurity puffs are used to obtain $[C^{6+},He^{2+}]_*=[C^{6+},He^{2+}]_{puff}$ -$[C^{6+},He^{2+}]_{background}$.

The first two plasma scenarios, denoted $S_1$ and $S_2$, were run at constant plasma current ($I_p$=0.9 MA), beam power ($P_{NBI}$= 1.8 MW) and toroidal magnetic field ($B_\phi$ = 0.5 T). $S_1$ is L-mode and $S_2$ is H-mode where the change was achieved by a change in the vertical position of the plasma; both plasmas maintained a double null magnetic geometry. The final scenario, denoted $S_3$, was based on $S_1$ but with $I_p$=0.6 MA. Helium is injected into $[S_1,S_2]$ and carbon into $[S_1,S_3]$.

The 2D imaging diagnostic [4] on MAST simultaneously captures both $C^{6+}$ and $He^{2+}$ CXR spectral intensities. With electron temperature and density measurements from Thomson Scat-

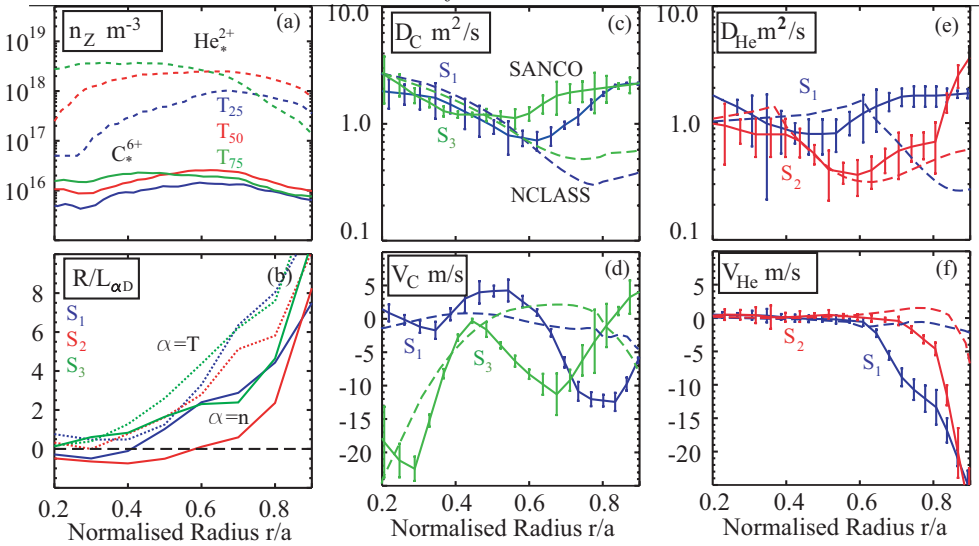


Figure 1: a) $C_*^{6+}$ and $He_*^{2+}$ densities obtained in $S_1$ for T-$T_{puff}$ = 25 (blue), 50 (red), 75 (green) ms. R/Ln$_D$ and R/LT$_D$ are given in b) for $S_1$ (blue), $S_2$ (red) and $S_3$ (green). $D_{C,He}$ and $V_{C,He}$ rates are plotted in c), e), d) and f) respectively for SANCO (solid) and NCLASS (dashed).

tering, effective CXR emission coefficients obtained from ADAS [5] are combined with theoretical predictions of the neutral beam density to convert the CXR emission into density.

**Results and Discussion**

The time evolution of $C_*^{6+}$ and $He_*^{2+}$ densities during $S_1$ are given in Fig. 1a. Good statistics of the rise and fall time of both species for normalised radius $0.2 < r/a < 0.9$ have been obtained. The SANCO code [6] solves the continuity equation with the 'standard ansatz' for particle flux, $\Gamma_Z = -D_Z \frac{\partial n_Z}{\partial r} + V_Z n_Z$, where $D_Z$ and $V_Z$ are varied to fit the evolution of the fully ionised radial impurity density, $n_Z$. Within $r/a < 0.5$ Fig. 1d and f show that both $V_C$ and $V_{He}$ are close to zero during $S_1$. Lowering $I_p$ causes an inward pinch of carbon as shown in Fig. 1d. Despite this change in $V_C$ at low $I_p$, $D_C$ remains virtually unchanged ($D_C \approx 1$ m$^2$/s) as shown in Fig. 1c.

For an assessment of the neoclassical transport, $D_Z$ and $V_Z$ calculated by NCLASS are overplotted in each case. The trends observed during the $I_p$ scan agree well with NCLASS results. The direction of the neoclassical convection is based on the balance of bulk ion density ($n_D$, simulated using TRANSP) and temperature ($T_D$, measured using CXR spectroscopy) gradient scale lengths (R/$L_{\alpha i}$=-R$\partial_r \ln \alpha_i$); the sign of the coefficient multiplying the latter can change therefore modifying the direction of $V_Z$. From Fig. 1b, it is seen that R/$L_{TD}$ remains constant within $r/a < 0.5$ while R/$L_{nD}$ changes sign from negative (outward) to positive (inward) at low $I_p$; this may account for the observed pinch.

Moving to $0.6 \leq r/a \leq 0.8$, anomalous rates of $D_{C,He}$ ($> 1$ m$^2$/s) and $V_{C,He}$ ($\sim$ -10 m/s) are

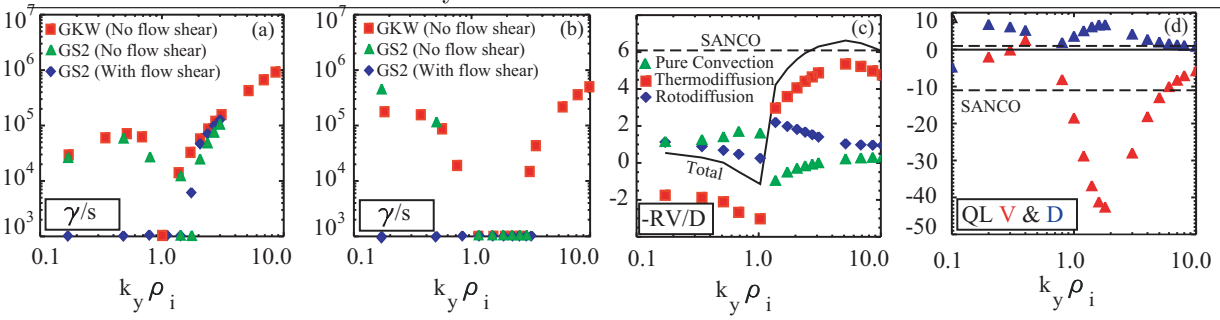


Figure 2: Gyrokinetic analysis performed at r/a=0.7. Linear growth rates as a function of wave number are shown for a) L-mode ($S_1$) and b) H-mode ($S_2$). In c), $-RV_C/D_C$ calculated from GKW is plotted for $S_1$ with the SANCO value (dashed). Quasi-linear scalings of $D_C$ (blue) and $V_C$ (red) are given in d) with SANCO values (dashed).

observed in L-mode. In this region, an increase in both $D_C$ and inward $V_C$ is observed as $I_p$ is decreased. Although the magnitude of $D_C$ is larger than NCLASS results, the observed trend is reproduced; NCLASS does not reproduce the trend nor the magnitude of $V_C$. Neoclassical levels of $D_{He}$ and $V_{He}$ are observed in H-mode suggesting that the microinstabilities responsible for the transport in L-mode are stabilised.

**Gyrokinetic Analysis**

An evaluation of the L- and H-mode linear microinstabilities at r/a=0.7 is conducted using GS2 and GKW codes. Both codes treat collisions differently which may cause differences to trapped electron modes (TEMs). It is seen from Fig. 2a that both GKW and GS2 predict positive (unstable) growth rates in good agreement for ion and electron scale modes with no flow shear included in both codes. A method was previously developed [7] to interpret the effect of the ExB flow shear and using this method with the experimental flow shear in the GS2 simulation it is found that ion scale growth rates ($k_y\rho_i < 1$) become stable.

Microinstabilities in H-mode are plotted in Fig. 2b. The main difference between L- and H-mode is the absence in H-mode of unstable TEMs within the region, $1 < k_y\rho_i < 3$, where $k_y$ is the wavenumber and $\rho_i$ the ion larmor radius. At low $R/L_{ne}$ in the H-mode plasma, the electron collision rate is sufficient to stabilise TEMs, as described in [7], and produce a stable region in the wavenumber spectrum $1 < k_y\rho_i < 4$.

Lastly, a comparison with experiment is made of the dimensionless impurity density profile peaking factor, written as

$$\frac{-RV_Z}{D_Z} = -C_T\frac{R}{L_{nz}} - C_u u'_Z - C_p, \qquad (1)$$

where $u'_Z$=-$(R^2/v_Z^{th})d\omega/dr$ with $\omega$ the plasma angular rotation frequency and $v_Z^{th}$ the impurity

thermal velocity. The three dimensionless coefficients are thermo-diffusion ($C_T$), roto-diffusion ($C_u$) and pure convection ($C_p$); the latter comprising the net effect of parallel compression and curvature. For trace species, $C_T$, $C_u$ and $C_p$ are determined using the method described in [8].

The three components which comprise $RV_C/D_C$ are plotted in Fig. 2c for $S_1$. Good agreement is found with the SANCO value between $2 < k_y\rho_i < 3$. Carbon has a larmor radius 2.5x smaller than deuterium and is expected to feel perturbations in this range. It should be noted that $C_T$, $C_u$ and $C_p$ reverse sign from their usual directions for ITG turbulence because of the change of mode frequency for TEM; here $C_T$ and $C_u$ both contribute to the observed inward pinch while the pure convection causes a subtle correction. Fig. 2d gives quasi-linear estimates of $D_C$ and $V_C$, where the perturbation amplitude is chosen to match the electron heat flux. Values within an order of magnitude of experiment are seen for $D_C$ and $V_C$ in the TEM region.

**Conclusions**

Perturbative carbon and helium gas puff experiments have been performed on MAST during two point plasma current and confinement mode scans. Transport coefficients deduced from the SANCO code have been compared with neoclassical results from NCLASS and gyrokinetic analysis with GS2 and GKW. The results show that impurity diffusivity and convection within $r/a < 0.5$ can be described by neoclassical theory in both L- and H-mode discharges. Trapped electron modes dominate the transport between $0.6 \leq r/a \leq 0.8$ in L-mode but these modes are stable in H-mode as the density gradient is lower and electron collisionality is higher. The inward pinch is thought to be caused by the thermo- and roto-diffusive terms dependent on the impurity temperature and rotation gradient respectively. The net transport caused by parallel compression and curvature described by the pure convection term causes only a subtle correction to the inward pinch. This work was funded by the RCUK Energy Programme and EURATOM. Simulations made on the HECTor super-computer were funded by EPSRC.

**References**

[1] W. Houlberg *et al*, Phys. Plasmas **4**, 3230 (1997)

[2] M. Kotschenreuther, G Rewoldt and W. M. Tang, Comput. Phys. Commun. **88** 128 (1995)

[3] A. G. Peeters *et al*, Comput. Phys. Commun. **180** 2650 (2009)

[4] A. Patel, P. G. Carolan and N. J. Conway, Rev. Sci. Instrum., to be submitted

[5] Atomic Data Analysis Structure, online at <http://adas.phys.strath.ac.uk>

[6] L. Lauro-Taroni *et al*, Proc. 21st EPS Conf., Montpellier, **1** 102 (1994)

[7] C. Roach *et al*, Plasma Phys. Cont. Fus. **51** 124020 (2009)

[8] F. J. Casson *et al*, Nucl. Fusion, **53** 063026 (2013)